reaction pathway. The second pathway, however, involves a prior coupling of one ditolylacetylene and acetylide to give a C_4 fragment similar to that observed in complex **4c**, followed by the reaction with a second ditolylacetylene and cleavage of the C–C bond to give the triply bridging alkylidyne and the C_5 alkylidene moiety.

We prefer the alkylidyne carbide pathway because the time period required for the reaction with ditolylacetylene (2.5 h) is much greater than that with dialkyl acetylenedicarboxylate (30 min), suggesting that the structure of the intermediate of the ditolylacetylene reaction (carbide + alkylidyne) may differ from that of complex 4 produced from reactions with dialkyl acetylenedicarboxylate. The greater reaction period also implies that the activation barrier of inducing the cleavage of the acetylide C–C bond is slightly higher than that of the coupling with dialkyl acetylenedicarboxylate. Furthermore, reactions of **4b** with excess ditolylacetylene or diethyl acetylenedicarboxylate under conditions similar (110 °C, 2.5 h) to those for the ditolylacetylene reaction have also been carried out; only decomposition was observed for these two reactions.

Although the alkylidyne carbide mechanism seems preferable, we still cannot completely eliminate the second possibility, because one may argue that the electron-withdrawing substituents of complex 4 would inhibit the reaction with the second alkyne and the following C–C bond cleavage reaction. Therefore, it would be useful if we could synthesize an analogous cluster complex that possesses the basic structure of **4c** but lacks the electron-withdrawing groups. The direct reaction of **1a** with exactly 1 equiv of ditolylacetylene has proved useless for this propose; therefore, we decided to approach the synthesis of this target molecule by using a triosmium alkyne complex and a metal acetylide. Unfortunately, the designated reaction between the unsaturated $Os_3(CO)_9(C_2Tol_2)$[24] and $CpW(CO)_3(C{\equiv}CPh)$ gives two new W–Os_3 clusters, neither of which has the expected geometry of complex **4c**. The results of these studies will be reported separately.

Acknowledgment. We are grateful to the National Science Council of the Republic of China for financial support (Grant No. NSC 79-2008-M007-52).

Supplementary Material Available: ORTEP diagrams for complexes **4c** and **5a** with a complete atomic labeling scheme and tables of nonessential bond distances and angles and anisotropic thermal parameters for **4c** and **5a** (14 pages); listings of the observed and calculated structure factors for **4c** and **5a** (29 pages). Ordering information is given on any current masthead page.

(23) Nucciarone, D.; Taylor, N. J.; Carty, A. J. *Organometallics* **1986**, *5*, 1179.

(24) Tachikawa, M.; Shapley, J. R.; Pierpont, C. G. *J. Am. Chem. Soc.* **1975**, *97*, 7172.

Mechanism of Hydride Fluxionality as Intramolecular Proton Transfer between Metal–Metal Bonds. Kinetics of Hydride Fluxionality for $(\mu\text{-H})_n\text{Ru}_3(\mu_3\text{-X})(\text{CO})_8\text{L}$ (n = 1, X = CH_2SEt, L = CO; n = 2, X = $CHCO_2Me$, $MeOC_2Me$, L = CO; n = 2, X = $CHCO_2Me$, L = PPh_3)

Leigh R. Nevinger and Jerome B. Keister*

Department of Chemistry, University at Buffalo, State University of New York, Buffalo, New York 14214

Received January 2, 1990

The kinetics of hydride fluxionality have been measured for the structurally analogous series of clusters $(\mu\text{-H})_n\text{Ru}_3(\mu_3\text{-X})(\text{CO})_8\text{L}$, in which the number of hydride ligands and the nature of the capping ligand can be varied. For $(\mu\text{-H})_2\text{Ru}_3(\mu_3\text{-CHCO}_2\text{Me})(\text{CO})_9$, the lower energy process ($\Delta H^\ddagger$ = 49.5 ± 7.6 kJ, $\Delta S^\ddagger$ = −4 ± 29 J/(K mol)) involves movement of one hydride to the Ru–Ru bond and the higher energy process ($\Delta H^\ddagger$ = 56.9 ± 5.9 kJ, $\Delta S^\ddagger$ = −33 ± 18 J/(K mol)), which exchanges the hydrides, is proposed to occur through a two-step pathway. Only hydride exchange is observed for $(\mu\text{-H})_2\text{Ru}_3(\mu_3\text{-CHCO}_2\text{Me})(\text{CO})_8(\text{PPh}_3)$ ($\Delta H^\ddagger$ = 53.9 ± 3.8 kJ, $\Delta S^\ddagger$ = −41 ± 12 J/(K mol)) and $(\mu\text{-H})_2\text{Ru}_3(\mu_3\text{-MeOC}_2\text{Me})(\text{CO})_9$ ($\Delta H^\ddagger$ = 54.0 ± 5.2 kJ, $\Delta S^\ddagger$ = −37 ± 19 J/(K mol)). The fluxional process for $(\mu\text{-H})\text{Ru}_3(\mu_3\text{-CH}_2\text{SEt})(\text{CO})_9$ consists of hydride exchange between the two metal–metal vectors which are bridged by carbon and sulfur ($\Delta G^\ddagger$ = 51 kJ at 248 K); the deuterium kinetic isotope effect was determined to be 1.6 (79% deuterium enrichment). Activation parameters and deuterium isotope effects for these compounds, in combination with literature values for a number of Ru_3 clusters, are rationalized in terms of the model of intramolecular proton transfer between metal–metal bonds via a transition state that contains a single terminal hydride ligand.

Introduction

It has been recognized for many years that hydride ligands on metal clusters are frequently involved in intramolecular migrations with rates on the order of the NMR time scale.[1] Although numerous studies of this dynamic behavior have been performed, it has not been possible to determine the relationship between the rate of hydride migration and the structure of the cluster. In fact, for clusters of greater than two metal atoms, in no case has it been possible to determine whether hydride migration proceeds through terminal or μ_3 coordination of the hydride ligand in the transition state.[39] The dynamics of hydride migration on metal clusters may be presumed to

(1) Band, E.; Muetterties, E. L. *Chem. Rev.* **1978**, *78*, 639. Evans, J. *Adv. Organomet. Chem.* **1977**, *16*, 319.

0276-7333/90/2309-2312$02.50/0

be a factor of great importance in the chemical reactivity of clusters. In recent studies, our group has proposed that hydride migration is involved in the mechanisms of ligand substitution,[2] reductive elimination of molecular hydrogen,[3] and reductive elimination of C–H bonds from trimetallic clusters.[4]

It was of interest, therefore, to determine the dynamic behavior of hydride ligands on Ru_3 clusters and the ways in which the kinetics of hydride migration are influenced by the structure of the cluster. In pursuit of this goal we have determined the kinetics of hydride fluxionality for the related clusters $(\mu\text{-}H)Ru_3(\mu_3\text{-}CH_2SEt)(CO)_9$,[5] $(\mu\text{-}H)_2Ru_3(\mu_3\text{-}CHCO_2Me)(CO)_9$,[6] $(\mu\text{-}H)_2Ru_3(\mu_3\text{-}CHCO_2Me)(CO)_8(PPh_3)$,[7] and $(\mu\text{-}H)_2Ru_3(\mu_3\text{-}MeOC_2Me)(CO)_9$,[8] a structurally analogous series in which the number of hydride ligands and the nature of a capping ligand can be varied. For each member of the series the crystal structure has been previously determined, including location of the hydride ligands by X-ray methods. In each case we have determined the nature of the migratory process(es) involving the hydride ligands, the rates for the NMR-detectable dynamic behavior, the activation parameters, and in one case the deuterium kinetic isotope effect. The migratory processes occurring for these clusters are compared with the behavior of two other Ru_3 cluster systems: $(\mu\text{-}H)_3Ru_3(\mu_3\text{-}CX)(CO)_9$ (X = H, alkyl, aryl, halide, and others), which show no dynamic behavior at room temperature, and $H(\mu\text{-}H)Ru_3(CO)_{11}$,[9] one of the few examples of a cluster in which bridging and terminal hydrides exchange. These comparisons lead to general conclusions regarding hydride mobility on clusters. The kinetics are rationalized in terms of a model involving intramolecular proton transfer between metal–metal bonds.

Experimental Section

The clusters $(\mu\text{-}H)Ru_3(\mu_3\text{-}CH_2SEt)(CO)_9$,[5] $(\mu\text{-}H)_2Ru_3(\mu_3\text{-}CHCO_2Me)(CO)_9$,[6] $(\mu\text{-}H)_2Ru_3(\mu_3\text{-}CHCO_2Me)(CO)_8(PPh_3)$,[7] and $(\mu\text{-}H)_2Ru_3(\mu_3\text{-}MeOC_2Me)(CO)_9$[8] were prepared by previously reported methods. Variable-temperature ^1H and ^{13}C NMR spectra were obtained on a JEOL FX-90Q fourier transform spectrometer; $Cr(acac)_3$ (0.02 M) was added as a relaxation agent for the ^{13}C NMR spectra. Mass spectra were recorded on a VG 70-SE mass spectrometer by Dr. Alice M. Bergmann and Gary Jones.

$(\mu\text{-}D)Ru_3(\mu_3\text{-}CH_2SEt)(CO)_9$. Attempts to prepare this deuterium-labeled cluster by pyrolysis of $(\mu\text{-}D)_3Ru_3(\mu_3\text{-}CSEt)(CO)_9$ were thwarted by scrambling of the deuterium with the support during thin-layer chromatography of the product on silica.

Method 1. A solution of $(\mu\text{-}H)Ru_3(\mu_3\text{-}CH_2SEt)(CO)_9$ (50 mg, 0.079 mmol) in THF (25 mL) was prepared in a 50-mL Schlenk flask under nitrogen. To this solution was added triethylamine (25 μL, 0.18 mmol) and D_2O (2 mL), both deoxygenated with a stream of nitrogen gas. The mixture was stirred under nitrogen at room temperature for 8 h. The solvent was removed by vacuum transfer. The extent of deuterium labeling in the hydride position was determined by ^1H NMR spectroscopy to be 61% by integration of the methylene proton resonance (2.47 ppm) of the ethyl group vs the hydride resonance (−16.58 ppm). Attempts to increase the deuterium labeling of the hydride position by repeated treatments with triethylamine and D_2O caused decomposition of the cluster.

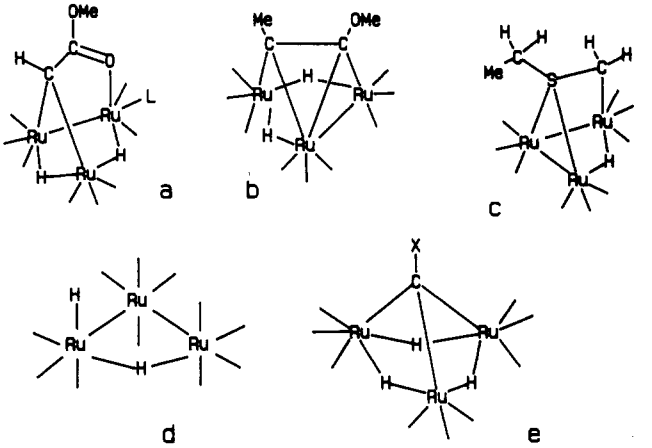

Figure 1. Structures for $(\mu\text{-}H)_2Ru_3(\mu_3\text{-}CHCO_2Me)(CO)_8L$ (L = CO, PPh_3) (a), $(\mu\text{-}H)_2Ru_3(\mu_3\text{-}MeOCCMe)(CO)_9$ (b), $(\mu\text{-}H)Ru_3(\mu_3\text{-}CH_2SEt)(CO)_9$ (c), $H(\mu\text{-}H)Ru_3(CO)_{11}$ (d), and $(\mu\text{-}H)_3Ru_3(\mu_3\text{-}CX)(CO)_9$ (e).

Method 2. A small amount of potassium hydride (5–6 mg) was added to a solution of $(\mu\text{-}H)Ru_3(\mu_3\text{-}CH_2SEt)(CO)_9$ (50 mg, 0.079 mmol) in THF (50 mL), and the solution was stirred under nitrogen for 8 h. At this point the IR spectrum of the solution showed only the presence of $K[Ru_3(CH_2SEt)(CO)_9]$. The solution was filtered under nitrogen to remove excess potassium hydride. Then the solvent was removed by vacuum transfer and the remaining solid was washed with two 10-mL portions of D_2O. The solid material was dried under vacuum and then washed with two 10-mL portions of dry *n*-hexane. The remaining solid was dissolved in THF (25 mL) containing trifluoroacetic acid-*d* (0.5 mL, 6.5 mmol), and the solution was stirred under nitrogen for 10 h at room temperature. The solvent was removed by vacuum transfer, leaving the deuterium-labeled product as the residue. The product was purified by washing a solution of the cluster in cyclohexane (25 mL) with two 10-mL portions of methanol. The yellow powder of $(\mu\text{-}D)Ru_3(\mu_3\text{-}CH_2SEt)(CO)_9$ showed 79% enrichment by ^1H NMR spectroscopy and mass spectrometry.

Kinetic Measurements. ^1H and ^{13}C NMR spectra were recorded on a JEOL FX-90Q multinuclear Fourier transform NMR spectrometer. Temperatures were measured via the methanol chemical shift method, accurate to ±1 °C.[10] ^1H NMR line shapes were calculated by using the program DNMR3.[11] ^{13}C NMR spectra were calculated by using a two-site exchange model (BASIC version written by W. D. Jones, University of Rochester; rewritten in Quickbasic 2.0 by J.B.K.) for each of the four pairs of exchanging resonances and for one static pair and then summing the five sets of spectra to give the complete spectrum at each temperature. Calculated spectra were visually compared with the experimental spectra to obtain rate constants at each temperature. Activation parameters were calculated from a least-squares determination (KINPLOT, written by Dr. Ronald Ruszczyk and modified by J.B.K.) of the slope and intercept of an Eyring plot of ln (k/T) vs $1/T$; error limits are given at the 95% confidence limits with use of Student's t values. It should be recognized that random errors in the experimental determinations of rate constants are expressed by the error limits of ΔH^* and ΔS^* but systematic errors due to, for example, incorrect assessment of temperature-dependent chemical shifts or incorrect estimates of line widths in the absence of exchange are not considered.

(2) Shaffer, M. R.; Keister, J. B. *Organometallics* **1986**, *5*, 561.
(3) Keister, J. B.; Onyeso, C. C. O. *Organometallics* **1988**, *7*, 2364.
(4) Duggan, T. P.; Muscatella, M. J.; Barnett, D. J.; Keister, J. B. *J. Am. Chem. Soc.* **1986**, *108*, 6076.
(5) Churchill, M. R.; Ziller, J. W.; Dalton, D. M.; Keister, J. B. *Organometallics* **1987**, *6*, 806.
(6) Churchill, M. R.; Janik, T. S.; Duggan, T. P.; Keister, J. B. *Organometallics* **1987**, *6*, 799.
(7) Janik, T. S.; Churchill, M. R.; Duggan, T. P.; Keister, J. B. *J. Organomet. Chem.* **1988**, *353*, 343.
(8) Churchill, M. R.; Fettinger, J. C.; Keister, J. B.; See, R.; Ziller, J. W. *Organometallics* **1985**, *4*, 2112.
(9) (a) Keister, J. B. *J. Organomet. Chem.* **1980**, *190*, C36. (b) Nevinger, L. R., Keister, J. B.; Maher, J. *Organometallics* **1990**, *9*, 1900.
(10) Van Geet, A. L. *Anal. Chem.* **1968**, *40*, 2227. Van Geet, A. L. *Anal. Chem.* **1970**, *42*, 679.
(11) Kleir, D. A.; Binsch, G. DMR3: A Computer Program for the Calculation of Complex Exchange-Broadened NMR Spectra. Modified Version for Spin Systems Exhibiting Magnetic Equivalence of Symmetry. *Quantum Chemistry Program Exchange*; Indiana University: Bloomington, IN, 1970; Program 165. Modified version by D. C. Roe (Du Pont Central Research) for use on a VAX computer and locally modified for use with DI-3000 graphics.

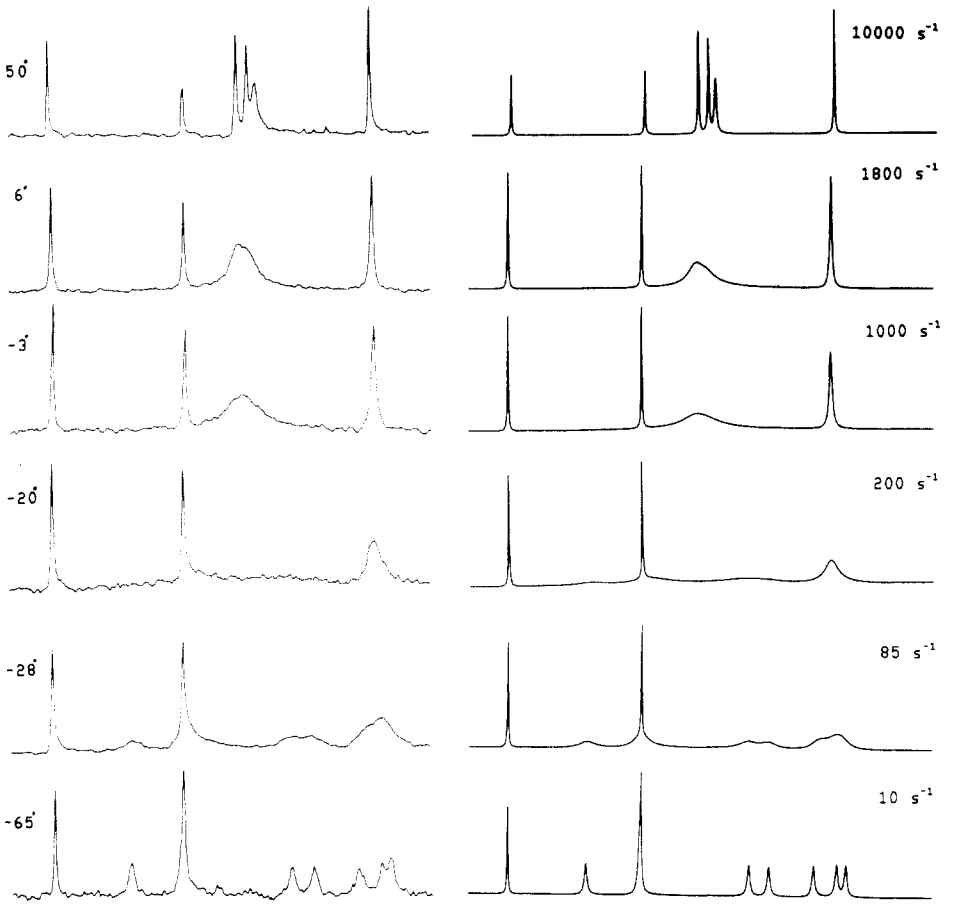

Figure 2. Experimental and calculated ^{13}C NMR spectra between 180 and 210 ppm for $(\mu\text{-H})_2Ru_3(\mu_3\text{-}CHCO_2Me)(CO)_9$. Temperatures are in °C.

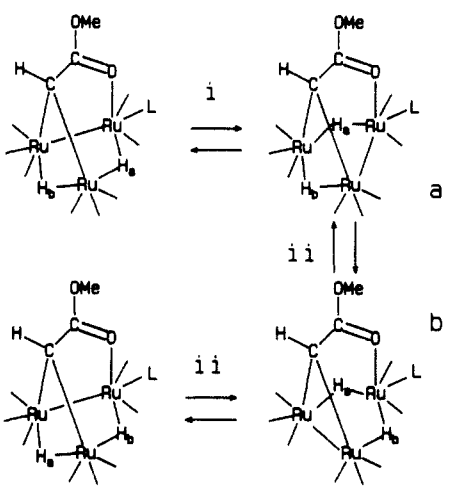

Figure 3. Proposed mechanism for the fluxional processes of $(\mu\text{-H})_2Ru_3(\mu_3\text{-}CHCO_2Me)(CO)_8L$ (L = CO, PPh_3).

Results

$(\mu\text{-H})_2Ru_3(\mu_3\text{-}CHCO_2Me)(CO)_9$. This molecule contains a $[Ru(CO)_3]_3$ framework capped by the $CHCO_2Me$ ligand (Figure 1a, L = CO).[6] One hydride bridges the edge of the Ru_3 triangle that is also bridged by carbon (Ru–H average distance 1.78 Å, Ru–H–Ru angle 104°); this hydride is located below the Ru_3 plane, relative to the capping ligand (dihedral angle 108°). The other hydride bridges an adjacent edge (Ru–H average distance 1.75 Å, Ru–H–Ru angle 116°) and is located in the Ru_3 plane (dihedral angle 182°). Two fluxional processes are observed.

The more facile fluxional process is observed by ^{13}C NMR spectroscopy. As described previously,[6] the ^{13}C NMR spectrum at 208 K contains eight signals between 150 and 210 ppm, representing nine carbonyl ligands and the acyl carbon, the signal at 197.6 ppm being due to the accidental overlap of three resonances. As the temperature of the sample is raised, eight of the carbonyl resonances are averaged in a pairwise manner to give four signals at 293 K (Figure 2); further narrowing of these signals occurs upon raising the temperature to 323 K. At 293 K the hydride resonances are only slightly broadened, indicating that the process responsible for the pairwise exchange of the CO resonances does not exchange the hydrides. The ^{13}C NMR spectrum at each temperature can be successfully simulated by using the same rate constant for exchange of each pair of carbonyls, indicating a common mechanism for exchange. This mechanism (Figure 3, L = CO, path i) is proposed to involve migration of hydride H_a to the unoccupied Ru–Ru edge, generating a plane of

Table I. Rate Constants for Hydride Migration

T, K	k, s^{-1}	T, K	k, s^{-1}	T, K	k, s^{-1}
		$H_2Ru_3(CHCO_2Me)(CO)_9$			
		(a) ^{13}C NMR Data			
245	85	270	1000	279	1800
253	200				
		(b) ^1H NMR Data			
283.8	3	307.8	35	368.4	1100
290.0	5	340.6	300	377.2	1700
298.6	20	359.2	900		
		$H_2Ru_3(CHCO_2Me)(CO)_8(PPh_3)$			
270.6	2	297.2	15	325.6	98
278.4	3	306.6	42	345.0	400
287.4	6	316.0	55	364.2	1100
		$H_2Ru_3(MeCCOMe)(CO)_9$			
242.2	8	260.0	74	306.2	3800
251.4	40	268.2	170	332.6	20000

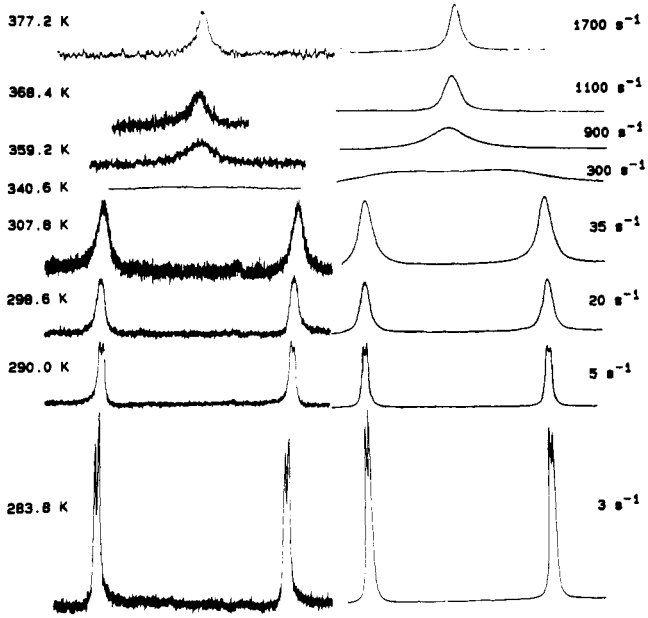

Figure 4. Experimental and calculated ^1H NMR line shapes for the hydride resonances of $(\mu\text{-}H)_2Ru_3(\mu_3\text{-}CHCO_2Me)(CO)_9$.

symmetry perpendicular to the Ru_3 plane and averaging the resonances for the CO ligands related by that symmetry. Rate constants are given in Table I. The activation parameters were calculated by using a computer-calculated least-squares procedure to determine the slope and intercept of the Eyring plot ($\Delta H^\ddagger$ = 49.5 ± 7.6 kJ (11.8 ± 1.8 kcal), $\Delta S^\ddagger$ = −4 ± 29 J/(K mol) (−1 ± 7 eu)). These values give rise to $\Delta G^\ddagger$(295 K) = 51 kJ/mol, in good agreement with the previously published estimated upper limit of 54 kJ/mol.[6]

At higher temperatures the ^1H NMR signals due to the hydrides broaden and eventually coalesce (Figure 4). At 377 K the coalesced resonance is broad, and decomposition of the compound prevented us from recording the limiting fast-exchange spectrum. The rate constants (Table I) for hydride exchange were calculated at each temperature, and the activation parameters were determined ($\Delta H^\ddagger$ = 56.9 ± 5.9 kJ (13.6 ± 1.4 kcal), $\Delta S^\ddagger$ = −33 ± 18 J/(K mol) (−7.8 ± 4.4 eu)). These data provide $\Delta G^\ddagger$(299 K) = 66.8 kJ/mol, in good agreement with the value obtained previously from line broadening.[6] The most likely mechanism for hydride exchange is migration of hydride H_b to the unoccupied Ru–Ru edge, followed by migration of hydride H_a to the Ru–Ru edge just vacated by H_b (Figure 3, L = CO, path ii).

$(\mu\text{-}H)_2Ru_3(\mu_3\text{-}CHCO_2Me)(CO)_8(PPh_3)$. The structure of this molecule is derived from that of $(\mu\text{-}H)_2Ru_3(\mu_3\text{-}CHCO_2Me)(CO)_9$ by substitution of the PPh_3 ligand for a CO ligand on the Ru atom to which the acyl is coordinated and in the equatorial coordination site cis to the bridging hydride (Figure 1a, L = PPh_3).[7] Coordination geometries of the hydride ligands are very similar to those of the hydrides of $(\mu\text{-}H)_2Ru_3(\mu_3\text{-}CHCO_2Me)(CO)_9$ (dihedral angles 97 and 183°). Since the isomer in which the PPh_3 ligand is trans to the bridging hydride is not observed (Figure 3, structure a), the only fluxional process that can be monitored by NMR spectroscopy is exchange of the two hydrides.

^1H NMR spectra were recorded from 270 to 364 K (Figure 1S, supplementary material). At 364 K the coalesced resonance is broad, and decomposition of the compound prevented us from recording the limiting fast-exchange spectrum. Rate constants (Table I) for the exchange at each temperature were determined, and the

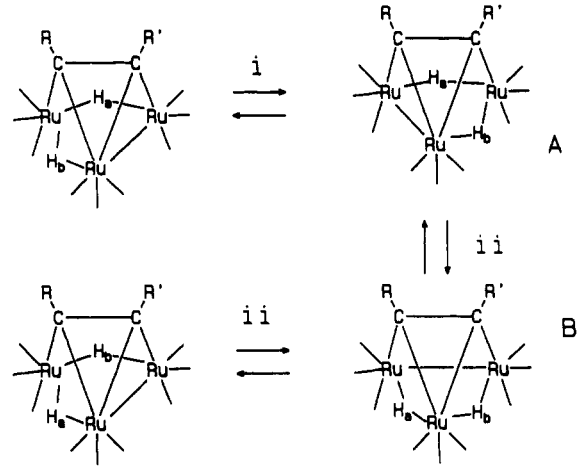

Figure 5. Proposed mechanism for hydride exchange on $(\mu\text{-}H)_2Ru_3(\mu_3\text{-}MeOCCMe)(CO)_9$.

activation parameters were calculated ($\Delta H^\ddagger$ = 53.9 ± 3.8 kJ (12.9 ± 0.9 kcal), $\Delta S^\ddagger$ = −41 ± 12 J/(K mol) (−9.7 ± 3.0 eu)). The mechanism for the hydride exchange in the substituted cluster should be the same as that for the parent cluster (Figure 3, L = PPh_3). The first step of the proposed mechanism is the movement of hydride H_a to the unoccupied Ru–Ru edge, generating the less stable isomer a. Hydride H_b then moves to the Ru–Ru edge just vacated by H_a, generating the still less stable intermediate b. Movement of H_a to the unoccupied Ru–Ru edge completes the exchange mechanism.

$(\mu\text{-}H)_2Ru_3(\mu_3\text{-}MeCCOMe)(CO)_9$. This cluster belongs to a series of extensively studied molecules of the formula $(\mu\text{-}H)_2M_3(\mu_3\text{-}RC_2R')(CO)_9$ (M = Ru, Os). In this cluster (Figure 1b) one hydride bridges the two Ru atoms that are σ-bonded to the MeC_2OMe ligand and lies in the plane of the Ru_3 triangle (average Ru–H distance 1.66 Å, Ru–H–Ru angle 116°, dihedral angle 174° between the RuHRu and Ru_3 planes); the other hydride, which bridges between one Ru atom that is σ-bonded to the MeC_2OMe ligand and the one Ru atom that is π-bonded to that ligand, lies below the Ru_3 plane (average Ru–H distance 1.73 Å, Ru–H–Ru angle 119°, dihedral angle 103°).[8] There are four fluxional processes that have been established in clusters of this class, particularly in Os systems.[12] The lowest energy process involves the movement of hydride H_a (Figure 5, path i) to the unoccupied cluster edge (for $(\mu\text{-}H)_2Ru_3(\mu_3\text{-}MeC_2Me)(CO)_9$, 47.4 kJ/mol[12c]). Hydride exchange (Figure 5, path ii) occurs with a higher activation barrier (for $(\mu\text{-}H)_2Ru_3(\mu_3\text{-}MeC_2Me)(CO)_9$, 57.7 kJ/mol). Other workers[12b] found little variation in $\Delta G^\ddagger$ for hydride exchange (ca. 48 kJ/mol) in Ru clusters with differing alkyl substituents R and R', although these data are significantly different from values obtained in the earlier study. Other fluxional processes are axial–radial CO exchange and alkyne "face flipping".

The kinetics of hydride exchange on $(\mu\text{-}H)_2Ru_3(\mu_3\text{-}MeCCOMe)(CO)_9$ were determined from the variable-temperature ^1H NMR spectra (Figure 2S, supplementary material). Because the isomer in which the hydride bridges the Ru–Ru vector syn to the methoxy group is not observed, only hydride exchange can be monitored. The static spectrum is obtained at 227 K. As the temperature is raised, the two hydride signals broaden and then dis-

(12) (a) Deeming, A. J. *J. Organomet. Chem.* **1978**, *150*, 123. (b) Aime, S.; Bertoncello, R.; Busetti, V.; Gobetto R.; Granozzi, G.; Osella, D. *Inorg. Chem.* **1986**, *25*, 4004. (c) Evans, J.; McNulty, G. S. *J. Chem. Soc., Dalton Trans.* **1981**, 2017.

Table II. Free Energies of Activation for Hydride Fluxionality on $H_nRu_3(X)(CO)_8L$ Clusters[a]

cluster	ΔG^*_1, kJ	ΔG^*_2, kJ	ref
$HRu_3(CH_2SEt)(CO)_9$	51[b]		
$H_2Ru_3(CHCO_2Me)(CO)_9$	50.7	66.6	
$H_2Ru_3(CHCO_2Me)(CO)_8(PPh_3)$		65.9	
$H_2Ru_3(CHCN\text{-}i\text{-}Pr_2)(CO)_9$	38	46.9	37
$H_2Ru_3(MeC_2OMe)(CO)_9$		63.8	
$H_2Ru_3(MeC_2Me)(CO)_9$		47.3[c]	12b
$H_2Ru_3(MeC_2Et)(CO)_9$		46.0[c]	12b
$H_2Ru_3(EtC_2Et)(CO)_9$		49.0[c]	12b
$H_2Ru_3(MeC_2Pr)(CO)_9$		48.1[c]	12b
$H_2Ru_3(C_8H_{12})(CO)_9$		49.4[d]	30
$H_2Ru_3(C_8H_8)(CO)_9$		51.5	31
$H_2Ru_3(MeCCMe)(CO)_9$	47.4[e]	57.7[f]	12c
$H_2Ru_3(CO)_{11}$		52[k]	9
$H_4Ru_4(CO)_{10}(dppe)$	30[g]		32
$H_4Ru_4(CO)_{10}(dppe)$		50.0[h]	35
	50.2[i]		33
$H_3Ru_4(CO)_{12}^-$		39.1 (42.4)[j]	34

[a] At 298 K unless otherwise noted. [b] 248 K. [c] Temperature was not reported. [d] 264 K. [e] 233 K. [f] 313 K. [g] 162 K. [h] This process involves exchange of three hydrides. The free energy is calculated from measured activation parameters: $\Delta H^* = 53.6$ (±2.5) kJ/mol, $\Delta S^* = 12$ (±9) J/(K mol). [i] Calculated from measured activation parameters: $\Delta H^* = 74$ (±4) kJ/mol, ΔS^* 80 (±16) J/(K mol), error limits given as 1 standard deviation. [j] Two models were used to calculate the line shapes and determine the rate constants. From these models activation parameters were determined. The first number is for one model, while the number in parentheses is for the second model: $\Delta H^* = 48.1$ (42.7) kJ/mol, $\Delta S^* = 30$ (1) J/(K mol). [k] 248 K.

appear into the base line. At elevated temperatures the signals coalesce and then sharpen to a singlet. Rate constants (Table I) for the exchange were calculated at each temperature, and the activation parameters were determined ($\Delta H^* = 54.0 \pm 5.2$ kJ (12.9 ± 1.2 kcal), $\Delta S^* = -37 \pm 19$ J/K mol (−8.8 ± 4.6 eu). The activation parameters give rise to ΔG^*(298 K) of 65 kJ/mol, somewhat higher than values determined for other $(\mu\text{-H})_2Ru_3(\mu_3\text{-alkyne})(CO)_9$ clusters (Table II).

$(\mu\text{-H})Ru_3(\mu_3\text{-}CH_2SEt)(CO)_9$. The structure (Figure 1c)[5] of this cluster contains a $[Ru(CO)_3]_3$ framework capped by a μ_3-CH_2SEt ligand in a geometry very similar to that found for $(\mu\text{-H})_2Ru_3(\mu_3\text{-}CHCO_2Me)(CO)_9$ above. The single hydride bridges the Ru atom bound to carbon and one of the Ru atoms bound to sulfur and is located in the Ru_3 plane (dihedral angle between the Ru_3 plane and the RuHRu plane, 171.3°, Ru–H(av) distance 1.7 Å, Ru–H–Ru angle 117°). The low symmetry of the molecule should produce nonequivalent methylene protons; however, at room temperature each pair of methylene proton resonances appears as a single resonance. At 208 K the methylene protons of the SEt group are shown to be nonequivalent; although the protons of the methylene group that is bound to Ru are also diastereotopic, apparently there is not a significant difference between the chemical shifts of these two, since only a broad singlet is observed. Rate constants for the hydride exchange were calculated by following the line-shape change of SEt methylene proton resonances. Due to the complex nature of the $AA'B_3$ spectra, line-shape fitting was much more difficult than for the other examples. The free energy of activation was calculated to be 51 kJ (12.2 kcal) at 248 K. A mechanism that would account for the observed spectra is the exchange of the hydride between the two Ru–Ru edges bridged by carbon and sulfur; this would generate an apparent plane of symmetry bisecting the methylene protons (Figure 6).

To determine the deuterium kinetic isotope effect upon hydride fluxionality, we prepared the labeled cluster

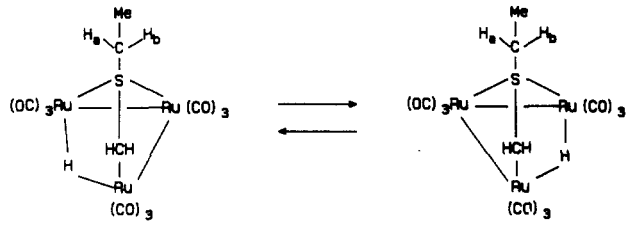

Figure 6. Proposed mechanism for the fluxional processes of $(\mu\text{-H})Ru_3(\mu_3\text{-}CH_2SEt)(CO)_9$.

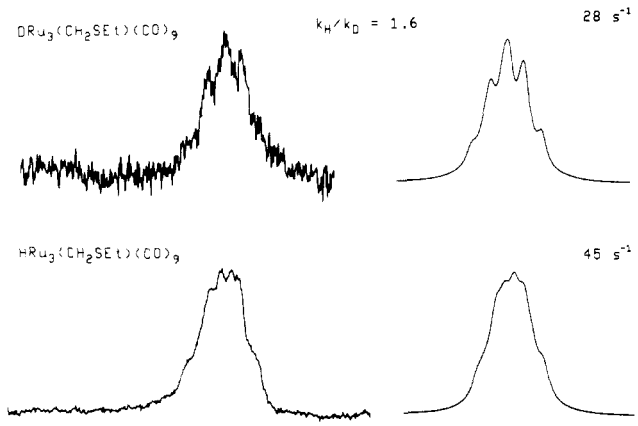

Figure 7. Experimental and calculated ^1H NMR line shapes for the methylene resonances of the SEt moiety of $(\mu\text{-H})Ru_3(\mu_3\text{-}CH_2SEt)(CO)_9$ and $(\mu\text{-D})Ru_3(\mu_3\text{-}CH_2SEt)(CO)_9$ at 248 K.

$DRu_3(CH_2SEt)(CO)_9$ (79% deuterium enrichment). The static spectrum for the methylene protons of the SEt moiety was identical with that of the unlabeled cluster. Spectral simulation of the methylene proton resonances gave the best match for $k = 28$ s^{-1}, vs 45 s^{-1} for the unlabeled cluster (Figure 7), giving the kinetic isotope effect (k_H/k_D) as 1.6 (estimated error limits ±0.3) at 248 K. No correction has been made for the ^1H content in the labeled sample.

Discussion

The hydride ligand displays its widest range of coordination modes on metal clusters. Examples of terminal, doubly bridging (the most common), triply bridging, and interstitial coordination are known. However, the factors that determine the ground-state configuration are not understood. It still is not possible to theoretically predict the coordination geometry adopted by a hydride ligand on a given cluster.

Although numerous instances of hydride fluxionality have been identified, the mechanism(s) and rate behavior are still poorly understood. Previous studies have measured activation barriers for hydride migration that range from 13 kJ to greater than 80 kJ. In many instances, hydride migration is coupled with migration of a carbonyl or other ligand type, thus confusing the issue of the nature of the mechanism and rate behavior. Relatively few determinations of activation enthalpies and entropies have been performed. It has been assumed that hydride fluxionality occurs through a change in coordination mode of the hydride between doubly bridging and either terminal or triply bridging, similar to mechanisms proposed for CO fluxionality. In fact, fluxional exchange of two or more hydrides has frequently been proposed to occur by simultaneous opening of two or more hydride bridges in a mechanism analogous to the Cotton mechanism for bridge–terminal CO exchange.[1,29]

Structure–reactivity relationships have played an important role in the determination of organic and inorganic

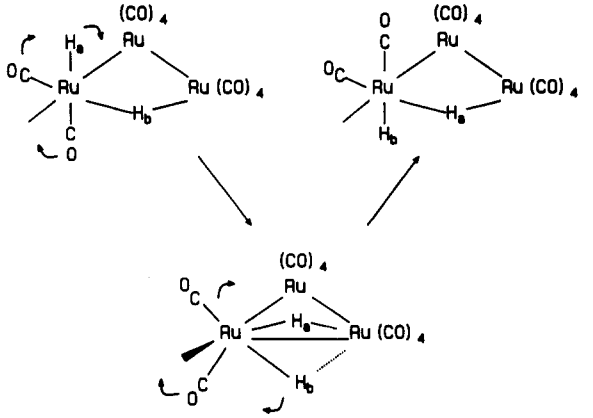

Figure 8. Proposed mechanism for hydride exchange on $H(\mu\text{-}H)Ru_3(CO)_{11}$.

reaction mechanisms. In this work we have used the systematic variation in the kinetics of dynamic NMR processes to probe the mechanism of hydride migration on $(\mu\text{-}H)_nRu_3(\mu_3\text{-}X)(CO)_8L$.

Relative Rates for Hydride Fluxionality. To compare the hydride fluxionality of the clusters, the free energy of activation for each dynamic process was calculated at 298 K for the clusters examined here, as well as some related clusters (Table II). The second column contains free energies of activation, $\Delta G^{\ddagger}_1$, for fluxional processes that involve movement of only one hydride ligand. The third column, $\Delta G^{\ddagger}_2$, contains entries for fluxional processes in which two or more hydrides are exchanging. It should be noted that a number of these values are obtained only from coalescence temperatures, that for several of the entries the nature of the fluxional process(es) is complicated by possible motions of other ligands, and that agreement between values measured for the same compound in different laboratories is only fair. Few measurements of activation parameters of simple hydride migrations have been made, and these are frequently of uncertain precision.

Nevertheless, some general observations can be made from these free energy of activation data for the Ru_3 clusters. The range of values is surprisingly small, considering the variations in the capping ligands and numbers of hydrides. Activation barriers are always slightly higher for exchange of two hydrides. The similarities of the values for hydride exchange suggest that the variations in electronic characteristics of the Ru_3 core, induced by changes in the ligand sphere (cf. entries 1 and 2 or 2 and 3 in Table II), have only a weak influence upon the hydride migration. Entropies of activation for the three examples studies here are all small and negative (average −30 J/(K mol)), certainly consistent with intramolecular processes.

The fluxional behavior of clusters containing both bridging and terminal hydride ligands provides some insight into the importance of the coordination geometry of the hydride ligand during the migratory process. The mechanism for hydride fluxionality on $H(\mu\text{-}H)Ru_3(CO)_{11}$ (Figure 1d)[9] is proposed to be analogous to that for $H(\mu\text{-}H)Os_3(CO)_{10}L$.[13] This exchange mechanism (Figure 8) invokes a turnstilelike motion of two carbonyl ligands and two hydride ligands about the metal–CO axis to generate an intermediate state with equivalent hydrides. On the basis of the variation in $\Delta G^{\ddagger}$ with the steric and electronic properties of L, Shapley and Keister[13a] have proposed that

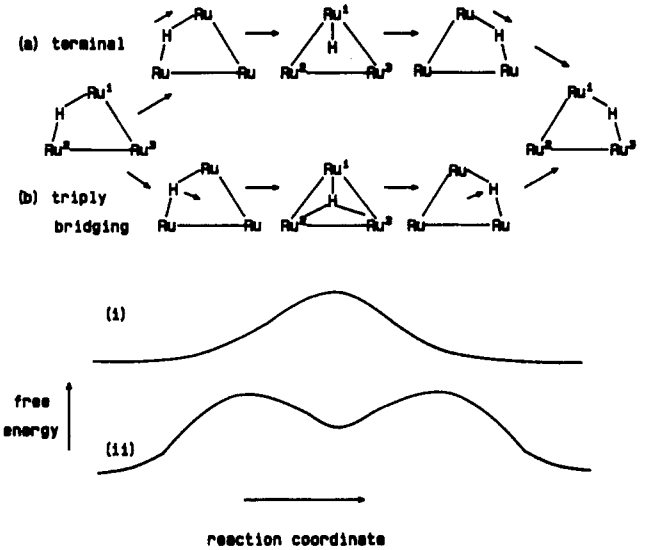

Figure 9. Pathways for migration of a single hydride from one Ru–Ru vector to another via a midpoint containing (a) a terminal or (b) a μ_3-hydride and either single (i) or double (ii) potential energy barriers. Structures in (a) and (b) correspond to the relative free energies along the reaction coordinate in (i) and (ii).

both hydrides are partially bridging in this intermediate state; however, Rosenberg and co-workers[13b] favor terminal coordination for both hydrides. We will have more to say about this later. Because one hydride ligand is terminally coordinated, the mechanism of hydride exchange in the $H(\mu\text{-}H)M_3(CO)_{11}$ systems differs from those of other entries in Table II which involve the exchange of two hydrides in that movement of only one hydride from a bridging to a terminal (or terminal to bridging) coordination site is sufficient to equilibrate both hydrides in a single elementary step. It is therefore notable that the free energy of activation for hydride exchange in $H(\mu\text{-}H)Ru_3(CO)_{11}$ is very similar to values for migrations involving only one hydride on a Ru_3 cluster.

The only entry in Table II for which hydride fluxionality is not observed is $(\mu\text{-}H)_3Ru_3(\mu_3\text{-}CX)(CO)_9$ (Figure 1e). Although the high symmetry of $(\mu\text{-}H)_3Ru_3(\mu_3\text{-}CX)(CO)_9$ prevents the observation of hydride exchange by ^1H NMR spectroscopy, the ^{13}C–^1H coupling between each hydride and the trans CO ligands of $(\mu\text{-}H)_3Ru_3(\mu_3\text{-}CMe)(CO)_9$ indicates a static structure at room temperature,[14] and the less symmetrical derivatives $(\mu\text{-}H)_3Ru_3(\mu_3\text{-}CX)(CO)_{9-n}(AsPh_3)_n$ (X = OMe, Ph, Cl)[15] and $(\mu\text{-}H)_3Ru_2Os(\mu_3\text{-}COMe)(CO)_9$[3] show sharp hydride resonances at higher temperatures.

The static nature of $(\mu\text{-}H)_3Ru_3(\mu_3\text{-}CX)(CO)_9$, in contrast to the fluxional behavior of all other Ru_3 clusters having at least one unbridged Ru–Ru bond, regardless of the number of hydride ligands or the nature of other ligands on the cluster, suggests that the mechanism for hydride migration requires at least one unbridged Ru–Ru bond. We therefore propose that in all cases the lowest energy pathway for hydride migration is a sequence of steps, each of which involves movement of a single hydride from a position bridging one Ru–Ru edge to an adjacent, unbridged Ru–Ru bond. If no such bond exists, no low-energy pathway for hydride exchange is available.

Hydride Fluxionality as Intramolecular Proton Exchange. Hydride fluxionality may be viewed as an

(13) (a) Keister, J. B.; Shapley, J. R. *Inorg. Chem.* **1982**, *21*, 3304. (b) Aime, S.; Osella, D.; Milone, L.; Rosenberg, E. *J. Organomet. Chem.* **1981**, *213*, 207.

(14) Forster, A.; Johnson, B. F. G.; Lewis, J.; Matheson, T. W. *J. Organomet. Chem.* **1976**, *104*, 225.

(15) Abdul Rahman, Z.; Beanan, L. R.; Bavaro, L. M.; Modi, S. P.; Keister, J. B.; Churchill, M. R. *J. Organomet. Chem.* **1984**, *263*, 75.

intramolecular proton exchange between two metal–metal bonds. Indeed, Fehlner and Housecroft have analyzed the structures and fluxionality of main-group/transition-metal clusters containing hydride bridges in terms of protonation of the site of maximum charge and have noted that "the greater the difference in availability of charge at potential sites, the greater the barrier to mobility."[16] The treatment of hydride migration between different metal–metal vectors as an intramolecular proton transfer may provide valuable insight into the dynamics of hydride ligands of cluster systems.

A proposed pathway for hydrogen migration from one Ru–Ru vector to another in an Ru_3 cluster is diagrammed schematically in Figure 9. We view this as a smooth transition in which the proton moves across the Ru_3 face with a continuous bonding interaction to at least one Ru atom, Ru(1). In the ground state Ru(1)–H and Ru(2)–H distances are ca. 1.7 Å, and the hydride may be either coplanar with the Ru_3 triangle or above the plane, but in either case the angle between the Ru_3 plane and the Ru(1)–H–Ru(2) plane is >90°.

At this point there is little information concerning the relationship between the free energy of activation for fluxionality and the dihedral angle between the Ru–H–Ru plane and the Ru_3 plane. That such a relationship may exist is suggested by the higher values of $\Delta G^{\ddagger}_1$ for $HRu_3(CH_2SEt)(CO)_9$ (51 kJ, dihedral angle 171°) and $H_2Ru_3(CHCO_2Me)(CO)_9$ (50.7 kJ, dihedral angle 182°), compared with the value of 38 kJ for $H_2Ru_3(CHCN\text{-}i\text{-}Pr_2)(CO)_9$[37] (dihedral angle ca. 160°, location determined indirectly). This comparison suggests that the free energy of activation may decrease as the dihedral angle between the Ru–H–Ru plane and the Ru_3 plane decreases, the coordination geometry of the hydride in the ground state moving along the proposed reaction coordinate in Figure 9. However, more examples need to be examined in which the rate of fluxionality can be related to the hydride geometry, which unfortunately can only very rarely be determined from X-ray crystallographic studies.

At the midpoint of the migration the hydride is symmetrically disposed between Ru(2) and Ru(3). If the transition state and the midpoint coincide, then the free energy diagram is as shown in Figure 9i with a single barrier. On the other hand, this may not in fact be the case, leading to a double barrier, as in Figure 9ii. The geometrical parameters of main interest are the three Ru–H distances. If the midpoint of the migration involves a terminal hydride (Figure 9a), then the Ru(1)–H distance will be shorter and the Ru(2)–H and Ru(3)–H distances very long. If the hydride interacts with all three metal atoms, then Ru(1)–H, Ru(2)–H, and Ru(3)–H distances will be approximately equal and longer than in the ground state (Figure 9b). Associated with hydride movement across the Ru_3 face will be rotation of the CO ligands to maintain approximate octahedral coordination for each Ru atom. The largest motion will be associated with the CO ligands most nearly in the Ru_3 plane. A rigid capping group, e.g. CH_2SEt, makes other structural changes small.

Rate–equilibrium relationships can provide a basis for understanding the rates of hydride mobility, which is treated as an intramolecular atom transfer.[17] Creutz and Sutin[18] have used the weak-interaction model for proton self-exchange to treat hydride exchange between mononuclear hydrides, such as $HMn(CO)_5$, and their conjugate bases. Hydride fluxionality should be more straightforwardly treated by this model than is intermolecular hydride transfer.

The weak-overlap model applied to proton transfer from an acid to a base expresses the free energy of activation, $\Delta G^{\ddagger}$, as given by eq 1, where $\Delta G°$ is the free energy change in the reaction and $\Delta G^{\ddagger}_0$ is the free energy of activation when $\Delta G° = 0$. The value of $\Delta G^{\ddagger}_0$ is given by eq 2, where

$$\Delta G^{\ddagger} = \Delta G^{\ddagger}_0(1 + \Delta G°/4\Delta G^{\ddagger}_0)^2 \approx \Delta G^{\ddagger}_0 + \Delta G°/2 \quad (1)$$

$$\Delta G^{\ddagger}_0 = W^r + (\lambda/4)[1 + (W^p - W^r)/\lambda]^2 \approx (W^r + W^p)/2 + \lambda/4 \quad (2)$$

$W^r = w^r - RT \ln (S^r s^r)$, w^r is the work required to bring the reactants together at the mean separation distance, S^r is a steric factor, and s^r is a statistical factor; equivalent definitions apply for the products, W^p. The term λ is the mean of the reorganizational barriers for the products and reactants, and $\lambda/4$ is the intrinsic contribution to the barrier for atom exchange.

For an intramolecular proton transfer from one basic site to another in a molecule with a low dipole moment and in a nonpolar solvent the work terms should be quite small, so $\Delta G^{\ddagger}_0$, the intrinsic free energy of activation, is approximately equal to $\lambda/4$. The major contributions to λ will come from the rearrangement necessary to bring the proton to the required position and the concomitant movement of the other ligands of the cluster. Solvent effects should be negligible, since hydrogen migration causes little, if any, change in charge distribution. Orientational effects are also expected to be small. A bridging hydride and an unbridged metal–metal bond both occupy a single coordination site of each metal; therefore, the coordination numbers of the metal atoms of the cluster do not change upon migration of a hydrogen atom from one metal–metal vector to another. Generally, cluster hydrides are more acidic than mononuclear hydride complexes, thus making exchange of the hydrogen as a proton even more favorable than is the case for intermolecular proton transfer.[19]

Relative rates for hydride fluxionality in related clusters, for which the intrinsic free energy barriers should be nearly the same, will thus be assumed to be determined by differences in the free energy minima in the migration reactions. Hydride migration may occur via single (Figure 9i) or double potential barriers (Figure 9ii). The two cases require different treatments since the free energy $\Delta G°$ associated with the latter is the free energy difference between the ground state and the intermediate (the value of which is likely to be close to that of $\Delta G^{\ddagger}$), whereas for the former case $\Delta G°$ is the free energy difference between the ground state and the product from the migration, a value close to zero.

First, the single potential energy barrier will be considered. In this case, $\Delta G° = 0$, so a single hydrogen migration from one metal–metal bond to another then has an activation barrier equal to the intrinsic kinetic barrier $\Delta G^{\ddagger}_0$ (e.g. 51 kJ/mol for migration of a single hydride ligand on $(\mu\text{-H})Ru_3(\mu_3\text{-}CH_2SEt)(CO)_9$ and $(\mu\text{-H})_2Ru_3(\mu_3\text{-}CHCO_2Me)(CO)_9$). However, for exchange of two hydride ligands we have postulated that two migrations, each an

(16) Housecroft, C. E.; Fehlner, T. P. *Organometallics* **1986**, *5*, 1279. Lynam, M. M.; Chipman, D. M.; Barreto, R. D.; Fehlner, T. P. *Organometallics* **1987**, *6*, 2405.

(17) (a) Marcus, R. A. *J. Phys. Chem.* **1968**, *72*, 891. (b) Kresge, A. J. *Acc. Chem. Res.* **1975**, *8*, 354. (c) Murdoch, J. R. *J. Am. Chem. Soc.* **1983**, *105*, 2159. (d) Grunwald, E. *J. Am. Chem. Soc.* **1985**, *107*, 125.

(18) Creutz, C.; Sutin, N. *J. Am. Chem. Soc.* **1988**, *110*, 2418.

(19) For information concerning pK_a values for metal hydrides: (a) Moore, E. J.; Sullivan, J. M.; Norton, J. R. *J. Am. Chem. Soc.* **1986**, *108*, 2257. (b) Edidin, R. T.; Sullivan, J. M.; Norton, J. R. *J. Am. Chem. Soc.* **1987**, *109*, 3945. (c) Kristjansdottir, S. S.; Moody, A. E.; Weberg, R. T.; Norton, J. R. *Organometallics* **1988**, *7*, 1983. (d) Walker, H. W.; Pearson, R. G.; Ford, P. C. *J. Am. Chem. Soc.* **1983**, *105*, 1179.

elementary step, are involved, and one of these must generate an intermediate that has a higher free energy than the ground-state structure. For that elementary step which generates the higher energy intermediate, the free energy of activation, given by eq 1, will be higher than the intrinsic barrier ΔG^*_0 by at least the amount $\Delta G°/2$ (and will be even greater if the intrinsic barrier is greater for this step). Application of eq 1 to exchange of the two hydrides on $(\mu\text{-H})_2Ru_3(\mu_3\text{-CHCO}_2\text{Me})(CO)_9$ would suggest that $\Delta G° <$ ca. 28 kJ/mol for isomerization of the ground-state structure to intermediate b in Figure 3. This is certainly within reason. This isomerization corresponds to proton transfer from a CRu–RuC bond to a CRu–RuO bond, and the basicity of a metal–metal bond is well-known to be strongly influenced by the ligands. The free energy for intermolecular proton transfer, which can be calculated from pK_a values[19] (and which has a high intrinsic barrier), can be used to provide estimates of the effects of ligand types upon ΔG^* for intramolecular hydrogen migration. For example, the acid–base reaction between $(\mu\text{-H})Fe_3(\mu_3\text{-SC}_6H_{11})(CO)_9$ (pK_a 16.9) and $[(\mu\text{-H})Fe_3(\mu_3\text{-PCMe}_3)(CO)_9]^-$ to give $[Fe_3(\mu_3\text{-SC}_6H_{11})(CO)_9]^-$ and $(\mu\text{-H})_2Fe_3(\mu_3\text{-PCMe}_3)(CO)_9$ (pK_a 11.4) has a $\Delta G°$ value of +31.4 kJ/mol, entirely attributable to the influence of the ligands attached to the Fe atoms associated with the metal–metal bond.[19c]

For the case of a double potential energy barrier, $\Delta G°$ in eq 1 is the difference in free energy between the ground state and the intermediate containing a terminal or triply bridging hydride ligand. Thus, the reaction is endothermic and the free energy of activation will be greater than the intrinsic value by at least $\Delta G°/2$. Variations in the relative rates for hydride migration may then be traced to changes in the relative energies of the intermediates that are induced by changes in the basicities of the metal–metal bonds as influenced by the ligand environments.

The utility of the model for the interpretation of structure–rate relationships for hydride fluxionality remains to be proven. Measurements of activation parameters for a range of structural classes wider than that presently available is necessary to test the limits of applicability of the model. Particularly desirable are examples in which the acidities of the M–H–M bonds may be correlated with rates for hydride fluxionality. The data presented in Table II unfortunately are primarily obtained from the class $(\mu\text{-H})_2Ru_3(\mu_3\text{-RCCR}')(CO)_9$ (entries 5–12), which would be expected to show only a small variation in rate for hydride fluxionality. As expected, the largest free energy of activation in this class is that for $(\mu\text{-H})_2Ru_3(\mu_3\text{-MeCCOMe})(CO)_9$, which has the most dissimilar alkyne substituents; the great difference in the properties of the substituents presumably increases the free energies of the intermediates A and B in the mechanism (Figure 5) relative to that of the ground-state structure and thus increases the free energy of activation.

One obvious goal of the application of the model would be to understand the variations in the rates of hydride migration with ligand substitutions. Unfortunately, ligand effects upon energy barriers for hydride fluxionality have been determined in very few instances.

Both steric and electronic effects were noted in the study of ligand effects on fluxionality in $H(\mu\text{-H})Os_3(CO)_{10}L$, with smaller and more basic ligands giving rise to faster rates.[13a] While the general features of the fluxional process are well understood (Figure 8), the question as to the nature of the bonding of the hydrides in the transition state remains unanswered. Rosenberg and co-workers[13b] favor terminal coordination for both hydrides in the transition state. If the transition state contains two terminal hydride ligands, then the electronic effects could be explained by the fact that in the ground state the $M(CO)_3L$ fragment is electron-rich (formally 18.5-electron metal center) while the $HM(CO)_3$ fragment is electron-poor (formally 17.5-electron metal center) but in the transition state both are 18-electron metal centers; good donor ligands L destabilize the ground state relative to the transition state. Steric effects may be explained by the observation that the steric interaction between L and the equatorial CO ligand on the adjacent metal atom is reduced if the cis metal–metal bond is bridged by a hydride ligand; this accounts for the fact that hydride bridges usually are found cis to phosphine ligands in substituted clusters.[36] Thus, in the $H(\mu\text{-H})Os_3(CO)_{10}L$ series there is a greater steric repulsion between L (the bulkiest ligand) and the CO ligands on the adjacent metal atoms in the transition state than in the ground state if the intermediate contains two terminal hydrides. On the other hand, Shapley and Keister[13a] have proposed that both hydrides are partially bridging in the transition state. If the transition state contains two bridging hydrides, then the electronic effects could be explained as being due to the stabilization of the M–H–M bonds by the higher electron density at the $M(CO)_3L$ fragment. The steric retardation of fluxionality could be explained by the higher coordination number at the $M(CO)_3L$ fragment in a transition state containing two hydride bridges. Thus, it has not been possible to use ligand effects to determine the nature of the transition state.

With respect to the influence of the ligands upon the activation barrier for exchange, it is interesting to compare the values for $(\mu\text{-H})_2Ru_3(\mu_3\text{-CHCO}_2\text{Me})(CO)_8L$ (L = CO, PPh_3). PPh_3 substitution for CO would be expected to increase the basicities of the metal–metal bonds to the $Ru(CO)_2L$ fragment, thus stabilizing intermediate b in Figure 3; however, due to steric effects PPh_3 substitution destablizes intermediate a relative to the ground-state structure and most likely would increase the intrinsic barrier due to rearrangement of the ligand sphere, as well. Apparently these effects cancel out in this instance.

Finally, the unusually low free energies of activation for $(\mu\text{-H})_3Ru_4(CO)_{12}^-$ and $(\mu\text{-H})_4Ru_4(CO)_{10}(dppe)$ must be considered. For tetrametallic clusters structures involving μ_3-H ligands have been proposed as intermediates in hydride exchange, and it is possible that the low values of ΔG^* for these clusters may signify a very different mechanism for fluxionality than that which occurs for the Ru_3 clusters. Alternatively, these lower barriers may reflect the effect of smaller dihedral angles between the Ru–H–Ru and Ru_3 planes in tetranuclear clusters.

The intrinsic barrier for hydride migration, ΔG^*_0, will be determined by a number of factors, including the energy required to reorganize the ancillary ligands, but the major contribution will come from the difference in the metal–hydrogen bond energies in the ground state and in the transition state. Unhappily, even the ground-state energies of metal–hydride bonds are poorly determined. The energy for disruption of the Ru–H–Ru bond of $(\mu\text{-H})_3Ru_3(\mu_3\text{-COMe})(CO)_9$, E(Ru–H–Ru), has been calculated to be 408 kJ/mol (derived by assuming E(Ru–Ru) = 115 kJ/mol[20]).[3] Although no determinations of terminal Ru–H bond energies have been performed, an estimate of 250 kJ/mol has been made.[21] Then the activation energy for

(20) Connor, J. A. In *Transition Metal Clusters*; Johnson, B. F. G., Ed.; Wiley: London, 1980; Chapter 5.

(21) (a) Pearson, R. G. *Chem. Rev.* **1985**, *85*, 41. (b) Halpern, J. *Inorg. Chim. Acta* **1985**, *100*, 41. (c) Sternal, R. S.; Sabat, M.; Marks, T. J. *J. Am. Chem. Soc.* **1987**, *109*, 7920.

Table III. Kinetic Isotope Effects for Hydride Migration

cluster	k_H/k_D
$H(\mu\text{-}H)Os_3(CO)_{10}(PPh_3)$	1.5 ± 0.1[a]
$(\mu\text{-}H)_2Ru_3(CO)_9(\mu_3\text{-}CH{=}CCMe_3)^{2+}$	1.44 (k_{HH}/k_{HD})[a]
	1.80 (k_{HH}/k_{DD})[a]
$(\mu\text{-}H)Ru_3(CH_2SEt)(CO)_9$	1.6[b]
$(\mu\text{-}H)_2M_3(\mu_3\text{-}S)(CO)_9$ (M = Ru, Os)	1.5–1.7[c]
$(\mu\text{-}H)_2Os_3(CO)_9(\mu_3\text{-}EtC_2Et)$	1.7[d]

[a] For exchange of two hydrides.[23] [b] This work. [c] Reference 35. [d] Reference 38.

conversion of a single Ru–H–Ru into a terminal Ru–H and an unbridged metal–metal bond is estimated as 43 kJ/mol, reasonably close to the activation enthalpy found for migration of a single hydride from one bridging position to another (e.g. $(\mu\text{-}H)_2Ru_3(\mu_3\text{-}CHCO_2Me)(CO)_9$, 50 kJ). However, since no information is available regarding the energy of a triply bridging $Ru_3(\mu_3\text{-}H)$ bond, the possibility of a triply bridging hydride cannot be eliminated on the basis of the activation parameters.

Kinetic Isotope Effects. One experiment that directly probes the nature of the transition state is the measurement of the deuterium kinetic isotope effect.[22] Deuterium kinetic isotope effects for hydride migration processes, introduced by Rosenberg and co-workers,[35] have been measured in only a few instances (Table III). Of the entries in Table III only that for $(\mu\text{-}H)Ru_3(\mu\text{-}CH_2SEt)(CO)_9$ concerns motion of a single hydride. Rosenberg et al. noted that the deuterium kinetic isotope effect (kie) for the exchange of the two hydrides of $(\mu\text{-}H)_2Ru_3(CO)_9(\mu_3\text{-}HCCCMe_3)^{2+}$, which they propose to occur via a two-step mechanism, is additive, so kie's for exchange of two hydrides are higher than those for processes involving only a single hydride.[23] We have previously measured k_H/k_D = 1.2 for isomerization of $(\mu\text{-}H)Ru_3(\mu\text{-}CNMe_2)(CO)_9(AsPh_3)$, proposed to involve hydride and $CNMe_2$ migration.[2] All kinetic isotope effects for hydride fluxionality that have been measured thus far are in the range 1–2.

Unfortunately, kinetic isotope effects are extremely difficult to interpret for such complicated systems. It has not been possible to use the previously measured kie values to distinguish between transition states in which the hydrogen is coordinated to one, two, or three metal atoms. Although the vibrational frequencies of the stretching modes for terminal ($\nu_{M\text{-}H}$ ca. 2000 cm^{-1}), μ-H ($\nu_{M\text{-}H\text{-}M}$ 1100–1700 cm^{-1}),[24a] and μ_3-H ($\nu_{M3\text{-}H}$ ca. 700 cm^{-1})[25] ligands are quite distinct, the transition state is certainly not linear, so contributions from other vibrational modes are likely to be more important, and the contribution from tunneling is unknown.[26]

The kinetic isotope effect k_H/k_D is given by eq 3, where $\nu_{H,g}$ and $\nu_{H,i}$ are the vibrational frequencies involving hydrogen in the ground and transition states, respectively.

$$\ln (k_H/k_D) = (0.187/T)\sum(\nu_{H,g} - \nu_{H,i}) \quad (3)$$

The application of this equation assumes that there is no contribution from tunneling and that no other vibrational modes are involved. Therefore, evaluation of k_H/k_D requires knowledge of the three vibrational frequencies involving hydrogen in the ground state and two frequencies in the transition state (the third corresponds to motion along the reaction coordinate). In a few cases all three frequencies have been determined for Ru–H, Ru–H–Ru, and $Ru_3(\mu_3\text{-}H)$ arrangements.

With use of very crude models the value of the kie expected for four extreme cases may be estimated. For the vibrational modes of the ground state $Ru_2(\mu\text{-}H)$ we will use the vibrational spectrum of $(\mu\text{-}H)_4Ru_4(CO)_9(P(OMe)_3)_4$[24] as a model. For early transition states (Figure 9ii) in which the vibrational modes are similar to those for the ground state, only the particular vibrational mode of the ground state that coincides with the reaction coordinate (either along the Ru–Ru vector or perpendicular to the Ru–Ru vector) will be considered. For symmetrical transition states (Figure 9i, either terminal or μ_3-hydride), the vibrational modes for the transition state can be approximated from the spectra of model compounds.

(1) If the transition state is an early one and the midpoint of the proton transfer involves a terminal hydrogen ligand, then the asymmetric stretch of the μ-H ligand will correspond roughly to motion along the reaction coordinate (Figure 9a,ii). If the other vibrational frequencies are similar in the ground and transition states, then only the asymmetric stretch (1190 cm^{-1}) need be considered and the value of k_H/k_D is expected to be ca. 2.4 at 250 K.

(2) If the transition state is an early one involving primarily the deformation mode (477 cm^{-1}) along the reaction coordinate (corresponding to the hydrogen moving over the face perpendicular to the Ru–Ru vector, as would be required to generate a μ_3-H ligand; Figure 9b,ii), then k_H/k_D would be expected to be ca. 1.4. However, because the potential well associated with the deformation is very shallow, it is not reasonable for this case to correctly model a transition state that is 50 kJ higher in energy than the ground state.

(3) On the other hand, if the transition state is similar to that described by a triply bridging ligand (Figure 9b,i), then the estimate can include all vibrational modes (with the spectrum of $(\mu_3\text{-}H)_2Ru_6(CO)_{18}$ as the model[25]), with one of the asymmetric stretching modes roughly corresponding to the reaction coordinate. On this basis

$$\ln (k_H/k_D) = (0.187/T)[(1620 - 710) + (1190 - 650) + 477]$$

$$k_H/k_D = 4.2 \text{ at } 250 \text{ K}$$

(4) A fourth extreme case, a transition state that can be described as a terminal hydrogen (Figure 9a,i), may also be considered. Stretching and bending vibrational modes have been identified for several mononuclear ruthenium hydrides, e.g. $RuHCl(CS)(PPh_3)_3$ (2027, 787 cm^{-1}),[27] $RuH_2(PPh_3)_4$ (2080, 820 cm^{-1}), and $H_4Ru(PPh_3)_3$ (1950, 805 cm^{-1}).[28] Here, a bending vibration (doubly degenerate)

(22) (a) Westheimer, F. H. *Chem. Rev.* **1961**, *61*, 265. (b) Saunders, W. H., Jr. Kinetic Isotope Effects. In *Investigation of Rates and Mechanisms of Reactions*; Lewis, E. S., Ed.; Wiley-Interscience: New York, 1974; Vol. 6, Part 1, p 211.

(23) Rosenberg, E.; Anslyn, E. V.; Barner-Thorsen, C.; Aime, S.; Osella, D.; Gobetto, R.; Milone, L. *Organometallics* **1984**, *3*, 1790.

(24) (a) For general references, see: Copper, C. B., III; Shriver, D. F.; Onaka, S. In *Transition Metal Hydrides*; Bau, R., Ed.; Advances in Chemistry 167; American Chemical Society: Washington, DC, 1978; Chapter 17, p 232. (b) For $(\mu\text{-}H)_4Ru_4(CO)_8[P(OMe)_3]_4$, ν_{sym} 1620 cm^{-1}, ν_{asym} 1190 cm^{-1}, ν_{def} 477 cm^{-1}: Orpen, A. G.; McMullan, R. K. *J. Chem. Soc., Dalton Trans.* **1983**, 463. (c) The vibrational spectrum of $(\mu\text{-}H)_3Ru_3(\mu_3\text{-}CX)(CO)_9$ has been analyzed, but the deformation modes were not identified: Oxton, I. A. *Spectrochim. Acta* **1982**, *38A*, 181.

(25) For $(\mu_3\text{-}H)_2Ru_6(CO)_{18}$, ν_{sym}(RuH) 710 cm^{-1} and ν_{asym} 650 cm^{-1} (doubly degenerate); Andrews, J. A.; Jayasooriya, U. A.; Oxton, I. A.; Powell, D. B.; Sheppard, N.; Jackson, P. F.; Johnson, B. F. G.; Lewis, J. *Inorg. Chem.* **1980**, *19*, 3033.

(26) for discussion of tunneling contribution to kie's on H_2 addition to Ir: Zhou, P.; Vitale, A. A.; San Filippo, J., Jr.; Saunders, W. H., Jr. *J. Am. Chem. Soc.* **1985**, *107*, 8049.

(27) Brothers, P. J.; Roper, W. R. *J. Organomet. Chem.* **1983**, *258*, 73.

(28) Harris, R. O.; Hota, N. K.; Sadavoy, L.; Yuen, J. M. C. *J. Organomet. Chem.* **1973**, *54*, 259.

(29) (a) Adams, R. D.; Cotton, F. A. *J. Am. Chem. Soc.* **1973**, *95*, 6589. (b) Cotton, F. A.; Hunter, D. L. *Inorg. Chim. Acta* **1974**, *11*, L9.

(30) Canty, A. J.; Johnson, B. F. G.; Lewis, J. *J. Organomet. Chem.* **1972**, *43*, C35.

corresponds most closely to the reaction coordinate. Taking the stretching vibrational frequency as 2000 cm^{-1} and the bending frequency as 800 cm^{-1}:

$$\ln (k_H/k_D) = (0.187/T)[(1620 - 2000) + (1190 - 800) + 477]$$

$$k_H/k_D = 1.4 \text{ at } 250 \text{ K}$$

Thus, at this point isotope effects do not provide enough information to distinguish between even these extreme examples presented above because of the low frequencies associated with the motion along the reaction coordinate. Of the models presented above, the one which most closely conforms to the experimentally determined activation parameters and kinetic isotope effects is that of a single potential energy barrier and a transition state containing a terminal hydride. Further measurements of temperature dependencies of the isotope effects and tritium kie's may provide the information necessary to more clearly define the nature of hydride fluxionality.

Conclusion

Hydride fluxionality on Ru_3 clusters occurs through a sequence of migrations, each involving the movement of a single bridging hydride ligand from one metal–metal vector to an adjacent unbridged metal–metal bond. The mechanism can be treated as a proton exchange from one metal–metal bond to another. The "intrinsic" free energies of activation are ca. 50 kJ/mol, with the other ligands in the coordination sphere having a minor influence due to steric and electronic effects. The kinetic isotope effects are ca. 1.5, and activation entropies are ca. −30 J/(K mol). The transition state containing a terminal hydride is consistent with the observed activation parameters and deuterium kinetic isotope effects.

Acknowledgment. This work was supported by the National Science Foundation through Grant CHE85-20276. We also acknowlege the Alfred P. Sloan Foundation. We thank T. Marder of the University of Waterloo for a copy of DNMR3 and W. Jones of the University of Rochester for the two-site exchange program. We gratefully acknowledge helpful discussions with A. G. Orpen (University of Bristol) and suggestions provided by Professors W. H. Saunders (University of Rochester) and E. Rosenberg (California State University, Northridge).

Supplementary Material Available: Figures 1S and 2S, giving observed and calculated ^1H NMR line shapes for $(\mu\text{-H})_2Ru_3(\mu_3\text{-}\eta^2\text{-CHCO}_2\text{Me})(CO)_8(PPh_3)$ and $(\mu\text{-H})_2Ru_3(\mu_3\text{-}\eta^2\text{-MeOC}_2\text{Me})(CO)_9$, respectively (2 pages). Ordering information is given on any current masthead page.

(31) Domingos, A. J. P.; Johnson, B. F. G.; Lewis, J. *J. Organomet. Chem.* **1972**, *36*, C43.
(32) Churchill, M. R.; Lashewycz, R. A.; Shapley, J. R. *Inorg. Chem.* **1980**, *19*, 1277.
(33) Shapley, J. R.; Richter, S. I.; Churchill, M. R.; Lashewycz, R. A. *J. Am. Chem. Soc.* **1977**, *99*, 7384.
(34) Koepke, J. W.; Johnson, J. R.; Knox, S. A. R.; Kaesz, H. D. *J. Am. Chem. Soc.* **1975**, *97*, 3947.
(35) Rosenberg, E. *Polyhedron* **1989**, *8*, 383.
(36) Farrugia, L. J.; Green, M.; Hankey, D. R.; Murray, M.; Orpen, A. G.; Stone, F. G. A. *J. Chem. Soc., Dalton Trans.* **1985**, 177.
(37) Rosenberg, E. Private communication.
(38) Bracker-Novak, J.; Hajela, S.; Lord, M.; Zhang, M.; Rosenberg, E.; Gobetto, R.; Milone, L.; Osella, D. *Organometallics* **1990**, *9*, 1379.
(39) For $(\mu\text{-H})_4Ru_4(CO)_{10}(PPh_2C_2H_4PPh_2)$, the ^1H NMR spectra have been interpreted to rule out the possibility of an intermediate containing four μ_3-H ligands, in favor of an intermediate containing four terminal hydrides.[33] However, this distinction depends upon an arbitrary assignment of one hydride resonance. Furthermore, the possibility of stepwise hydride migration via intermediates having μ_3-H ligands or terminal hydrides could not be ruled out.

Formation of an Agostic Bond by Protonation. Characterization by NMR Spectroscopy of $[(\mu\text{-H})_3M_3(\mu_3\text{-}\eta^2\text{-HCR})(CO)_9][SO_3CF_3]$ (M = Ru, R = Et, $CHPhCH_2Ph$; M = Os, R = Me)

David K. Bower and Jerome B. Keister*

Department of Chemistry, University at Buffalo, State University of New York, Buffalo, New York 14214

Received January 23, 1990

Protonation of $(\mu\text{-H})_3M_3(\mu_3\text{-CX})(CO)_9$ (M = Ru, X = Et, $CHPhCH_2Ph$; M = Os, X = Me) in HSO_3CF_3 solution yields $[(\mu\text{-H})_3M_3(\mu_3\text{-}\eta^2\text{-HCR})(CO)_9]^+$, in which the proton has been shown by ^1H and ^{13}C NMR spectroscopy to add across a C–M edge. The agostic hydrogen is fluxionally exchanged among all three C–M bonds but does not exchange with the bridging hydrides. These protonated clusters prove to be more susceptible to reductive elimination of CH_3X than their neutral precursors. When M = Ru and X = H, Cl, Br, and Ph, addition of acid causes immediate cluster decomposition. When X = Ph and $CHPhCH_2Ph$, the reductive-elimination products toluene and 1,2-diphenylpropane have been identified.

Introduction

We have proposed that the reversible formation of an intermediate containing an agostic bond is the first step in the reductive elimination of CH_3X from $(\mu\text{-H})_3Ru_3(\mu_3\text{-CX})(CO)_9$ under CO.[1] Reversible formation of an agostic bond by hydride migration from a metal–metal edge to a metal–carbon edge has been demonstrated in $Fe_3(CO)_9CH_4$, which exists in solution as an equilibrium mixture of tautomers $(\mu\text{-H})_3Fe_3(\mu_3\text{-CH})(CO)_9$, $(\mu\text{-H})_2Fe_3(\mu_3\text{-HCH})(CO)_9$, and $(\mu\text{-H})Fe_3(\mu_3\text{-H}_2CH)(CO)_9$; deprotonation yields $[(\mu\text{-H})Fe_3(\mu_3\text{-HCH})(CO)_9]^-$ (Figure 1).[2] However, $(\mu\text{-H})_3M_3(CO)_9(\mu_3\text{-CH})$ (M = Ru, Os) exists as the single isomer which contains no agostic bond. Also,

(1) (a) Duggan, T. P.; Barnett, D. J.; Muscatella, M. J.; Keister, J. B. *J. Am. Chem. Soc.* **1986**, *108*, 6076. (b) Duggan, T. P.; Golden, M. A.; Keister, J. B. *Organometallics* **1990**, *9*, 1656.

(2) Dutta, T. K.; Vites, J. C.; Jacobsen, G. B.; Fehlner, T. P. *Organometallics* **1987**, *6*, 842.

0276-7333/90/2309-2321$02.50/0